



**HAL**  
open science

## Stable dispersions of double-walled carbon nanotubes for carbon nanotube/copper co-deposition

Mauricio Pavía, Mélanie Emo, Fahad Alnjiman, Enrico Andreoli, Jean-François Pierson, Emmanuel Flahaut, Ewa Kazimierska, Brigitte Vigolo

### ► To cite this version:

Mauricio Pavía, Mélanie Emo, Fahad Alnjiman, Enrico Andreoli, Jean-François Pierson, et al.. Stable dispersions of double-walled carbon nanotubes for carbon nanotube/copper co-deposition. *Materials Chemistry and Physics*, 2023, 299, pp.127491. 10.1016/j.matchemphys.2023.127491 . hal-03987138

HAL Id: hal-03987138

<https://hal.univ-lorraine.fr/hal-03987138v1>

Submitted on 16 Feb 2023

**HAL** is a multi-disciplinary open access archive for the deposit and dissemination of scientific research documents, whether they are published or not. The documents may come from teaching and research institutions in France or abroad, or from public or private research centers.

L'archive ouverte pluridisciplinaire **HAL**, est destinée au dépôt et à la diffusion de documents scientifiques de niveau recherche, publiés ou non, émanant des établissements d'enseignement et de recherche français ou étrangers, des laboratoires publics ou privés.



Distributed under a Creative Commons Attribution - NonCommercial - NoDerivatives 4.0 International License

# Stable dispersions of double-walled carbon nanotubes for carbon nanotube/copper co-deposition

*Mauricio Pavía<sup>a</sup>, Mélanie Emo<sup>a</sup>, Fahad Alnjiman<sup>a</sup>, Enrico Andreoli<sup>b</sup>, Jean-François Pierson<sup>a</sup>, Emmanuel Flahaut<sup>c</sup>, Ewa Kazimierska<sup>b</sup>, Brigitte Vigolo<sup>a,\*</sup>*

<sup>a</sup> Université de Lorraine, CNRS, Institut Jean Lamour, F-54000 Nancy, France

<sup>b</sup> Swansea University, Energy Safety Research Institute, SA1 8EN Swansea, Wales, UK

<sup>c</sup> CIRIMAT, CNRS-INP-UPS, Université Toulouse 3 Paul Sabatier, 118 route de Narbonne, F-31062 Toulouse cedex 9, France

\*Corresponding author : Dr. Brigitte Vigolo; [Brigitte.Vigolo@univ-lorraine.fr](mailto:Brigitte.Vigolo@univ-lorraine.fr)

**Keywords** Double-Walled Carbon Nanotube; Dispersion; Surfactant; Co-electrodeposition; CNT-Cu composites

**Abstract:** This work explores a novel approach to disperse purified double-walled carbon nanotubes in high ionic strength aqueous media, *i.e.* a copper ion solution to further prepare double-walled carbon nanotubes/Cu composites by co-electrodeposition. Firstly, the metal catalyst

impurities in the tube samples are selectively removed by a one-pot gas-phase purification treatment. Two non-ionic (Triton X-100 and Pluronic-P123) and one anionic (sodium dodecyl sulfate) surfactant were used to disperse the purified samples by varying the carbon nanotubes/surfactant ratio and the surfactant content. Triton X-100 is a poly(ethylene glycol) in which one of the terminal hydroxy groups has been converted into the corresponding p-(2,4,4-trimethylpentan-3-yl)phenyl ether. Pluronic-P123 is a triblock copolymer comprising poly(ethylene oxide) (PEO) and poly(propylene oxide) (PPO) leading to PEO-PPO-PEO. Sodium dodecyl sulfate of chemical formula  $C_{12}H_{25}OSO_2ONa$  possesses a sulfate head and a hydrocarbon tail. The capability of each surfactant to disperse the double-walled carbon nanotubes in the copper ion solution is analyzed and later discussed based on the nature of the inter-tube forces. Among the employed surfactants, Pluronic-P123 exhibits the best dispersive level since stable and homogenous suspensions of double-walled carbon nanotubes are obtained. The dispersion mechanism proposes that the hydrophobic nature of Pluronic-P123 promotes efficient steric repulsions allowing the stable dispersion in the copper electrolyte. The samples dispersed by this way are successfully co-deposited and they form well-distributed double-walled carbon nanotubes within the copper matrix. The obtained results are an important step on the way to achieving an efficient double-walled carbon nanotubes/Cu composite synthesized by electrodeposition means.

## **1. Introduction**

Proper incorporation of carbon nanotubes (CNTs) in a copper matrix is of great interest as CNT/Cu composites have the potential to face the limitations of pure copper in terms of electrical and thermal properties. The best-known example of these limitations concerns electronics. In the race for device miniaturization and densification in order to transport, process and analyze more

and more data, pure copper will not be suitable anymore in the near future. CNTs combine high surface, low density and remarkable electronic properties. Electrical current density (defined as the current flowing through a conductor per unit cross-sectional area of the conductor) of single-walled CNTs (SWCNTs) and double-walled CNTs (DWCNTs) are of around  $10^9$  A cm<sup>-2</sup> and  $10^8$  A cm<sup>-2</sup><sup>1-4</sup>, respectively is 100 times higher than that of bulk Cu. CNTs have hence attracted great attention because their combination with copper has a high potential to become an efficient way to overcome copper limitations. Considering they combine exceptional characteristics of few-wall-number with the advantage to keep the inner tube intact in case of eventual damage to the outer wall, DWCNTs are considered as a particularly interesting class of CNTs<sup>5,6</sup>. Unfortunately, copper has a well-known very weak affinity with carbon-based materials. Consequently, proper integration of the carbon-based materials with a uniform distribution within a copper matrix and good interface interactions remains challenging. Besides, this very weak affinity avoids the formation of defined compounds at the CNT/Cu interface.

It is well established that the selection of the fabrication process could greatly impact the properties of the outcome CNT/Cu composites<sup>7</sup>. Nowadays the two main technologies used for fabricating CNT/Cu composites are powder processing and electrochemical deposition. In powder metallurgy, the two powders of metallic Cu and CNTs are mixed together by ball milling<sup>8</sup> or ultrasonication<sup>9</sup>, followed by compaction (sintering<sup>10</sup>, hot pressing<sup>11,12</sup>). The main limitation of this processing approach is the poor adhesion between the CNT surface and Cu leading to non-uniform composites after compaction; the CNTs forming large agglomerates instead of a good embedding within the copper matrix<sup>7,13</sup>. Moreover, these CNT/Cu composites shaped as macroscopic pellets<sup>14</sup> or wires<sup>15</sup> are not suitable for microscale composite structures required for many current electronic devices. On the other hand, the electrodeposition process is a low cost,

easy operation and well-controlled method which allows the formation of homogeneous and large-range thickness films of metal on any surface <sup>16,17</sup>. The properties of composites, such as CNT content and particle size can be easily controlled during deposition by varying the electrolyte chemistry, electrical regimes, etc. For example, the surface morphology of the films is affected by the current density. For example, a relatively smooth surface can be obtained at a low current density <sup>18</sup>. Co-deposition of CNTs and copper in a one-pot process to form CNT-Cu films <sup>19</sup> stands for a very attractive approach since it has the potential to lead to an homogeneous distribution of the CNTs and strong interface interactions between the CNT surface and copper <sup>13,20,21</sup>. A successful preparation of homogeneous CNT/Cu composites by co-electrodeposition strongly depends on the quality of the CNT dispersion in the plating solution. Indeed, CNTs are hydrophobic by nature and strongly tend to agglomerate into clusters because of attractive van der Waals forces between them. To improve the wettability of the hydrophobic surface of the tubes and to uniformly disperse them, it exists two common routes. The CNTs can be covalently functionalized. In that case, the introduced surface groups help to improve their dispersion in aqueous solvents. However, as is well known, covalent functionalization introduces defects in the CNT structure which diminishes their intrinsic properties and impedes an optimized benefit of their electrical conductivity in the final composite<sup>22-26</sup>. A less destructive and simpler method to disperse CNTs and stabilize their suspension in aqueous media is based on the use of surfactants. The surfactants help in decreasing the surface tension and free energy at the interface between the nanotubes and the electrolyte solution.

Ionic surfactants (sodium dodecylbenzene sulfonate (SDBS), sodium dodecyl sulfate (SDS), or hexadecyltrimethylammonium bromide (CTAB)) have been mostly used to disperse CNTs in past

co-deposition works <sup>27,28</sup>. In literature, non-ionic surfactants are seldom studied to disperse properly CNTs and used to form CNT/Cu composite by co-electrodeposition.

In previous works, scholars focused their studies mostly on functionalized multi-walled CNTs (MWCNTs) and SWCNTs and their dispersions with ionic surfactants. To the best of our knowledge, DWCNTs dispersed with Pluronic-P123 have not been co-electrodeposited with copper yet <sup>17</sup>.

In this work, we have dispersed high-stability purified DWCNTs in a copper sulfate electrolyte with the help of surfactants. Different kinds of surfactants, including anionic and nonionic, have been investigated by varying the DWCNT/surfactant ratio. The dispersion quality depending on the used surfactant and the CNTs and the surfactant concentration has been evaluated by direct visual observations, optical microscopy (OM) and ultraviolet-visible (UV-visible) spectrophotometry. The behavior of the prepared DWCNT dispersions in the copper sulfate solution (at pH 1) is discussed based on the inter-CNT forces occurring depending on the nature of the wetting-agent. Interestingly, the hydrophilic–lipophilic balance (HLB) of the used surfactants allows to strengthen the comprehensible mechanism proposed. A selected DWCNT dispersion because of its greater dispersion quality was used to co-electrodeposit the purified DWCNTs and copper. The obtained samples were first characterized by Raman spectroscopy. From Thermogravimetric analysis (TGA), we showed that a significant amount around 4.9 vol.% of DWCNTs was introduced within copper under its metallic state, confirmed by X-ray diffraction (XRD). Transmission and Scanning electron microscopy (TEM and SEM) served to put into evidence that undamaged DWCNTs are well embedded within the copper matrix. This work hence furnishes an innovative approach for a successful introduction of DWCNTs in copper matrix.

## **2. Materials and methods**

### **2.1 Materials**

The DWCNTs studied in this work were synthesized by a Catalytic Chemical Vapor Deposition (CCVD) process at the Centre Inter-Universitaire de Recherche et d'Ingénierie des Matériaux (CIRIMAT, Toulouse, France). Co and Mo were used as catalysts. The average diameter of the used DWCNTs is between 1.4 and 2.0 nm and their length up to 10  $\mu\text{m}$ <sup>29</sup>.

The protocol to prepare the  $\text{Cu}^{2+}$ /sulfuric acid ( $\text{H}_2\text{SO}_4$ ) solution (hereafter named the copper ion solution) was the following: first, 1 L of  $\text{H}_2\text{SO}_4$  at 0.05 M (pH 1) was prepared by diluting 2.81 mL of 98 %  $\text{H}_2\text{SO}_4$  in water. Then, 125 g of a copper sulfate pentahydrate ( $\text{CuSO}_4 \cdot 5 \text{H}_2\text{O}$ ) salt were added to achieve the desired final copper concentration of 0.5 M.

Pluronic-P123 (P123), Triton X-100 (TX100) and Sodium Dodecyl Sulfate (SDS) were purchased from Sigma Aldrich (Germany) and used as received.

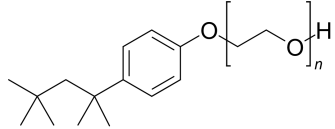
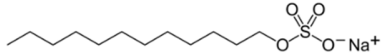
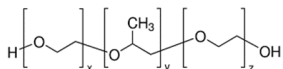
### **2.2 Experimental set-up**

Pristine DWCNTs were firstly purified by a chlorine gas-based method<sup>30</sup>, the experimental conditions are given in Figure S1 and Table S1, Supporting Information.

The purified DWCNTs were thereafter dispersed in the copper ion solution by using 3 different surfactants. First, for each surfactant, a mother solution of 4 wt.% of surfactant in the copper ion solution was prepared. The solutions were stirred for 16 h and let to settle for 12 h before their use. Then, the solutions were diluted until the desired surfactant concentration was achieved. Therefore the powdered DWCNTs purified was added to the surfactant/copper ion solution mixture and eventually diluted to prepare the samples listed in Table 1. To disperse the DWCNTs, the mixtures were stirred for 60 min in 1 s pulse mode at 35 % amplitude using a Cole-palmer 500-Watt

ultrasonic probe. Then, the samples were directly observed by optical microscopy to follow their dispersion state.

**Table 1.** DWCNT dispersion in the copper ion solution prepared with Pluronic-P123 (P123), Triton X-100 (TX100) and SDS as surfactant with the DWCNT/surfactant ratios.

Sample name	Surfactant	Chemical formula, complete name and chemical structure of the surfactant	Surfactant [wt.%]	Surfactant [mM/L]	DWCNT [wt.%]	DWCNT/surfactant (weight ratio)
ST1	TX100	$C_8H_{17}C_6H_4(OC_2H_4)_{9-10}OH$ polyethylene glycol p-(1,1,3,3-tetramethylbutyl)-phenyl ether	0.5	7.7	0.1	0.2
ST2	TX100		1.0	15.4	0.1	0.1
ST3	TX100		2.0	30.9	0.1	0.05
SS1	SDS		$NaC_{12}H_{25}SO_4$ sodium dodecyl sulfate	0.5	17.3	0.1
SS2	SDS		1.0	34.6	0.1	0.1
SS3	SDS		2.0	69.2	0.1	0.05
SP1	P123		$HO(CH_2CH_2O)_{20}(CH_2CH(CH_3)O)_{70}(CH_2CH_2O)_{20}H$	0.5	0.85	0.1
SP2	P123	poly (ethylene glycol)-block-poly (propylene glycol)-block-poly (ethylene glycol) $x,z=20$ $y=70$	1.0	1.7	0.1	0.1
SP3	P123			2.0	3.4	0.1

Once the OM analysis concluded, the samples were left to settle during 10 days to evaluate the dispersion endurance. OM observations were carried out with an Olympus TH4-200 BXS1



microscope. A drop of the DWCNT dispersion was deposited on a glass slide where a cover glass was first disposed, a second cover glass was placed on the sample so that the sample thickness can be chosen to optimize the observation quality. For simplification purpose, only the optical objective x10 was used. The shown OM micrographs of the DWCNT dispersions are those taken after 60 min of sonication.

### **2.3 Electrochemical deposition of DWCNT/Cu composites**

DWCNT/Cu composites were co-electrodeposited from a copper ion solution containing 0.1 wt.% of DWCNTs stabilised with 2.0 wt.% of Pluronic-P123 using a copper rod electrode ( $d=0.635$  cm, Goodfellow) as cathode and a platinum mesh as anode. Sulfuric acid was added to prevent the formation of copper oxides and adjust the electrolyte conductivity. Such a solution was stable for 8 weeks as observed with the naked eye.

To produce a homogenous suspension of DWCNTs in the electrolyte, the mixture was ultrasonically stirred for 60 min in 5 s pulse mode at 20 % amplitude using a Cole-Parmer 500-Watt ultrasonic homogenizer before the electrochemical co-deposition. To limit the intrinsic tendency of CNTs to agglomerate even over a short time, the plating solution was gently stirred during electrodeposition. Stirring ensures also the constant availability of copper ions in the vicinity of the surface of the working electrode.

Electrodeposition was carried out at room temperature in galvanostatic mode (IviumStat, Ivium Technologies) with a cathode current density varying in the 21.2 - 116 mA cm<sup>-2</sup> range till complete reduction of copper ions in 1000 steps. The optimal current density was selected at -69.6 mA cm<sup>-2</sup> and the effect of added Pluronic-P123 surfactant and DWCNTs on the electrodeposition process was analysed and further discussed. A homemade electrolytic cell, a glass sample vial (internal

dimension of 27.1 mm) with a snap closure lid was used for all depositions. The volume of the plating bath was 10 cm<sup>3</sup>. The holes were cut in the lid to allow the vertical insertion of electrodes. Additional vent holes were also cut to allow the excess of forming gases to escape from the cell. All potentials reported in this study are referred to Ag/AgCl/1.0 M KCl (0.222 V vs. SHE). The DWCNT/Cu composite powders were obtained by manual scraping from the cathode, a few powders were located at the cell bottom due to continuous agitation. Both powders were mixed together, filtered and thoroughly rinsed with deionized water, followed by drying in an oven at 80 °C overnight.

For comparison purpose, pure copper powders were also fabricated with the same electrolyte and the same deposition operating conditions but without adding the DWCNTs or DWCNTs and surfactant mixture to the copper ion solution.

OM, TEM and TGA analyses were carried out to analyze the DWCNT samples after purification and dispersion. Raman spectroscopy, TGA, XRD, TEM and SEM were used to further characterize the electrodeposited DWCNT/Cu samples. The experimental conditions used for each analysis are described below.

For the TEM observations, the raw and the purified DWCNTs and the DWCNT/Cu composite powder were dispersed in ethanol and gently sonicated in a sonication bath for 5 min. A droplet of the prepared DWCNT dispersion was then deposited on a copper grid covered with a holey amorphous carbon film (200 mesh size) provided by Delta Microscopies. The TEM micrographs were obtained in bright field mode using a JEOL JEM-ARM 200F apparatus quipped with a spherical aberration (Cs) probe corrector working at an accelerating voltage of 80 kV. In this work, the TEM figures were prepared with selected DWCNT images representative of each sample from

a batch of *ca.* 30 images obtained at different places randomly selected on the TEM grid for the same sample.

SEM was carried out with a ZEISS Gemini SEM 500 equipped with a field emission gun.

A Setaram Setsys evolution 1750 was used for TGA analysis. TGA was performed by increasing temperature from room temperature to 900 °C (5°C/min) under dry airflow (20 mL/min) for the raw and the purified DWCNTs as well as the electrodeposited samples.

Micro-Raman spectroscopy was carried out with a Jobin Yvon LabRAM HR800 equipped with a CCD detector cooled to -70 °C. A 633 nm laser wavelength was used as the incident beam focused on the sample with a microscope through a wide length x50 objective and a numerical aperture of 0.50. For each sample, at least 5 spectra were recorded from a different area on the sample. For each spectrum, the background was subtracted and the maximum intensity of the D and the G bands were used to calculate the D intensity over the G intensity ratio,  $I_D/I_G$ .

X-ray diffraction analyses were performed using a Bruker D8 Advance diffractometer in Bragg-Brentano configuration using a copper anticathode ( $\lambda K_{\alpha 1} = 0.15406$  nm).

Ultraviolet-visible (UV-visible) spectrophotometry study has been carried out with a Varian Cary7000 spectrophotometer in the 200-700 nm range by using quartz cuvettes (28-F/Q/10) purchased from Jasco France with an optical path of 2 mm. The absorbance of the dispersion SP3 was measured by using a double beam mode by substrating the absorbance of the reference sample (copper ion solution at pH 1 with 2 % of P123). Sample absorbance at 500 nm was used to follow its stability during 8 days<sup>31,32</sup>.

### **3 Results and discussion**

The procedure used to prepare the DWCNT/Cu composite is shown in figure 1. The raw DWCNTs are first purified under a chlorine stream during 2 h at 1000°C leading to remove a

significant proportion of their metal based impurities. The purified DWCNTs are dispersed in the acidic copper ion solution at a concentration of 0.1 wt.% with the help of Pluronic-P123 (2 wt.%) as surfactant and sonication. The dispersed DWCNTs are next simply transferred in the electrochemical cell to undergo the co-electrodeposition process forming the DWCNT/Cu composite.

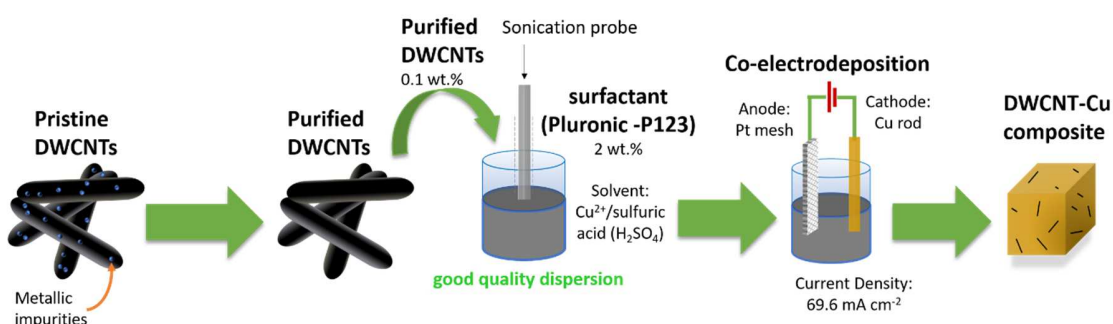


**Figure 1** Schematic of the procedure used to prepare the DWCNT/Cu composites by co-electrodeposition with Pluronic-P123 stabilized DWCNT dispersion in copper ion plating solution.

### 3.1 DWCNT dispersion

#### 3.1.1 Stability of DWCNTs in the copper ion solution: optimization of the surfactant type and concentration

Based on the works reported on the used chlorine-based purification method<sup>33–37</sup>, no or only a few amount of functional groups are expected to be present at the CNT surface since at the high used temperature (1000 °C), both chlorine- and oxygen-containing functional groups are unstable. The use of surfactant is then all the more essential to disperse these hydrophobic DWCNTs. They were dispersed in the copper ion solution by ultrasonic stirring in the presence of 3 different surfactants: Triton X-100, Sodium Dodecyl Sulfate and Pluronic-P123. In water or aqueous

solvents, ionic surfactants, induce long-range distance electrostatic repulsions between the covered surface of CNTs for their efficient dispersion<sup>38</sup>. Nonetheless, the copper electrolyte (acidified solution of copper sulfate) being a high ionic strength solution, charge screening by ions can dramatically affect the CNTs dispersion stability. This is the reason why non-ionic surfactants, such as Triton X-100 or Pluronic-P123, are here expected to be more relevant to successfully disperse CNTs in the copper electrolyte. Their presence on the CNT surface produces steric repulsions between the CNT walls to maintain them in a dispersed state. Understand the behavior of different natures of surfactant is crucial to successfully achieve a proper dispersion in the electrolyte.

$\zeta$ -potential measurements, commonly used to evaluate the dispersion state of colloidal solutions, would be not relevant when Triton X-100 and Pluronic-P123 are used since they do not lead to charged surfaces for the covered DWCNTs by these two nonionic surfactant. The weak dispersion ability of SDS to disperse the DWCNTs simply proved by visual and OM observations makes such investigation by the  $\zeta$ -potential technique unapropriate in that case. After their preparation, the dispersions were directly observed by OM and let to settle down during 10 days to qualitatively evaluate their stability. Figure 1 shows photographs of a selection of representative dispersions with the 3 used surfactants at the same weight concentration 10 days after their preparation.

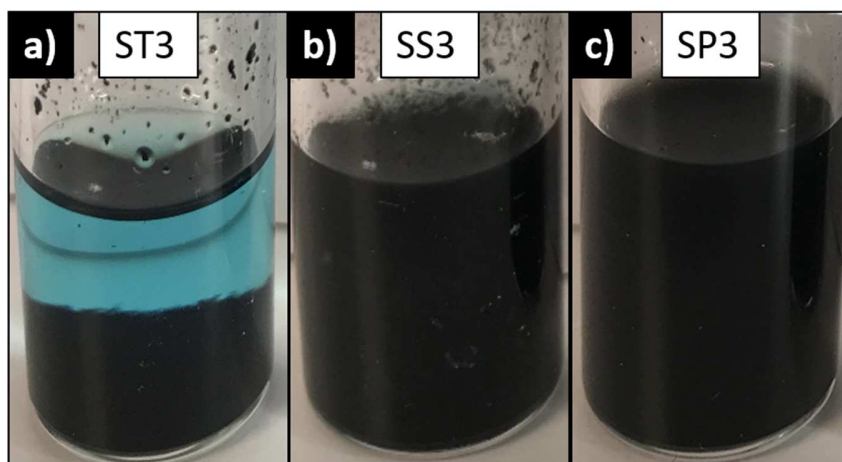


**Figure 2** Images of 3 different samples after 10 days of settling time. Prepared with 0.1 wt.% of purified DWCNTs with a) Triton X-100 at 2.0 wt.% (ST3), b) SDS at 2.0 wt.% (SS3), c) Pluronic-P123 at 2.0 wt.% (SP3).

The sample prepared with Pluronic-P123 (Figure 2c) differs from the dispersions prepared with Triton X-100 and SDS (Figures 2a and 2b). For these latter, a common characteristic is the presence of agglomerates on the internal vial walls and within the DWCNT suspension when SDS and Triton X-100 are used. In the case of Triton X-100 (Figure 2a), the DWCNT agglomerates are even sedimented at the bottom of the vials and well separated from the solvent noticeable with its blue typical color. For the sample prepared with Pluronic-P123, the DWCNT dispersion has a much more homogeneous aspect than that observed for the dispersions prepared with the two other surfactants. After 10 days, no sign of agglomeration was noticeable (Figure 2c).

The prepared DWCNT dispersions were systematically observed by OM (Figure 3). Even if the spatial resolution of an optical microscope is much larger than that required to evidence any individualized or even bundled DWCNTs, this technique is commonly used to assess CNT stability

as it reveals any agglomerate presence<sup>38,39</sup>. From OM observations, the solvent alone shows a transparent/yellow uniform color (microscope illumination), no trace of the typical blue color from the Cu solution is noticeable due to the weak thickness of the solution analyzed by OM. The DWCNT dispersions prepared with Triton X-100 (Figures 3a-3c) and with SDS (Figures 3d-3f) show a comparable aspect, *i.e.* more (Triton X-100) or less (SDS) dense flocculated structures. These DWCNT agglomerates probably come from a re-agglomeration phenomenon of previously dispersed DWCNTs within the surfactant/copper ion medium; no obvious behavior evolution with the surfactant concentration is noticed. In the case of the DWCNTs dispersed with Pluronic-P123 (Figures 3g-3i), the DWCNT agglomerates are observed in the form of small dark dots homogeneously distributed in the images. Contrary to the aspect observed for the DWCNT dispersions prepared with Triton X-100 and SDS, these dark dots certainly come from small residues not dispersed from the DWCNT solid powder while the main part of the DWCNTs is rather well dispersed as shown by the darker background of the image Figure 3i compared to others. The optimization of the used surfactant concentration is crucial for this work since a too high concentration would result in a foaming solution and would hinder the co-electrodeposition. On the contrary, a too weak surfactant concentration will not promote the dispersion of the CNTs. When the Pluronic-P123 concentration increases from 0.5 to 2.0 wt.%, the size and the number of these dense DWCNT agglomerates is reduced. This behavior is in agreement with what was observed in figure S2, Supporting Information.

In summary, from OM analysis, we have shown that DWCNT agglomeration or re-agglomeration easily occurs when Triton X-100 or SDS is used as surfactant while the DWCNT dispersions prepared with 1.0 and 2.0 wt.% of Pluronic-P123 are of relatively high quality.

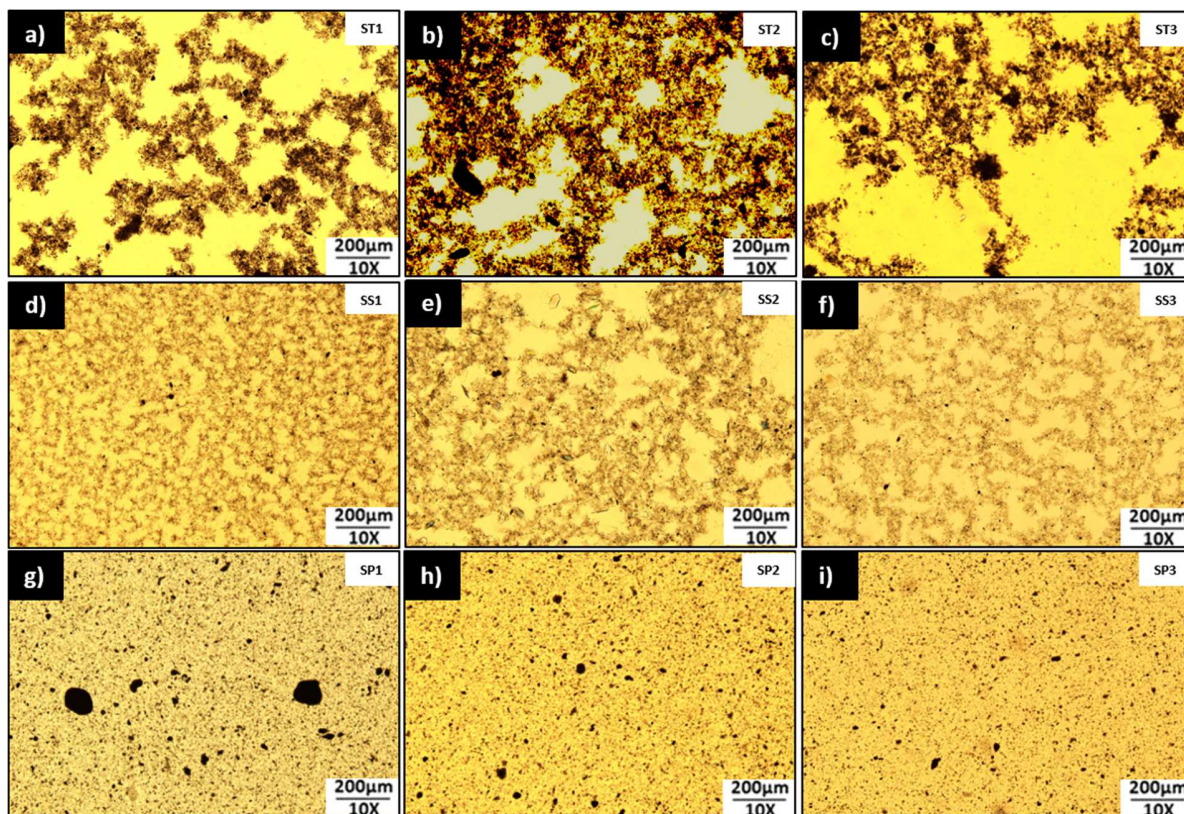


**Figure 3** OM images of the prepared DWCNT dispersions after 60 min of sonication with 0.1 wt.% of DWCNTs and different concentrations of surfactants: with Triton X-100 at concentrations of: a) 0.5 wt.% (ST1), b) 1.0 wt.% (ST2) and c) 2.0 wt.% (ST3); with SDS at concentrations of: d) 0.5 wt.% (SS1), e) 1.0 wt.% (SS2) and f) 2.0 wt.% (SS3) and prepared with Pluronic-P123 at concentrations of: g) 0.5 wt.% (SP1), h) 1.0 wt.% (SP2) and i) 2.0 wt.% (SP3).

The samples prepared with Pluronic-P123 which have shown the best ability to disperse the DWCNTs were centrifuged at 2500 rpm during 10 min. As it is shown in figure 4, only sample SP3 prepared with 2.0 wt.% of Pluronic-P123 does not show any sedimentation sign at simple sight, a recurrent mark of a good dispersion. For sample SP3, the resulting supernatant was taken and later characterized by UV spectrophotometry.



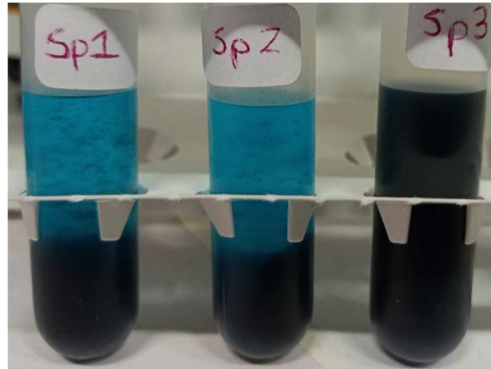


**Figure 4** Images of 3 different dispersions prepared with 0.1 wt.% of purified DWCNTs and Pluronic-P123 at different concentrations in the copper solution at Ph 1; SP1: 0.5 wt.%, SP2: 1.0 wt.% and SP3: 2.0 wt.% after being centrifuged at 2500 rpm during 10 min.

The dispersion stability of SP3 prepared with 0.1 wt.% of DWCNTs and 2.0 wt.% of Pluronic-P123 which was further used for copper-DWCNT coelectrodeposition was followed by UV-visible spectrophotometry without any dilution prior to the absorbance measurements. After a weak increment of absorbance, SP3 absorbance remains stable without significant reduction during the 8 day analysis, being the sign of minimum sedimentation and good stability (Figure 5).

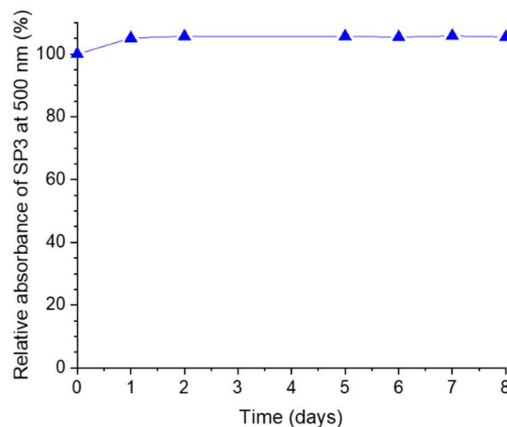


**Figure 5** Relative absorbance of SP3 (0.1 wt.% of purified DWCNTs and 2.0 wt.% of Pluronic-P123) after being centrifuged at 2500 rpm during 10 min.

### *3.1.2 Efficient repulsive interactions between DWCNTs with Pluronic-P123: proposed mechanism*

SDS, being an ionic surfactant, its weak ability to disperse DWCNTs in the copper ion solution is probably due to strong screening effects leading to create attractive forces between the DWCNT surface and thus their re-agglomeration<sup>31</sup>. Among the two used nonionic surfactants, Triton X-100 shows a lower DWCNT dispersion efficiency than Pluronic-P123. The dispersion of CNTs with the help of surfactants in water has been extensively studied since such homogeneously dispersed CNTs are often one of the key stages to process and include them in new designed materials<sup>40,41</sup>. The surfactant molecules adsorb onto the hydrophobic CNT surface and reduce the interfacial energy between the tubes and the solvent<sup>42,43</sup>. The surfactant concentration has to be high enough (typically above the Critical Micellar Concentration (CMC)) to guarantee a sufficient CNT covering. However, if the number of micelles is too high in the medium, attractive forces of depletion can appear and induce CNT dispersion destabilization<sup>31,38</sup>. These attractive interactions between the covered CNTs (large particles) are due to an osmotic pressure created by the micelles (small particles) on the CNTs. The higher the micelle concentration, the stronger the resulting depletion attractive forces. The optimized surfactant concentration window has to be found to favor a good CNT outer surface covering and consecutive CNT dispersion while avoiding their re-agglomeration. The surfactant ability to disperse the CNTs depends on the nature of the dispersion medium, the nature (and the concentration) of the surfactant which will govern its affinity with the nanoparticle surface. And its CMC will directly impact the coverage rate of the surfactant at the

nanoparticle surface. All these factors are important for obtaining an efficient dispersion of nanoparticles including CNTs by surfactants<sup>42,44,45</sup>. With such a number of factors, it is hard to predict the behavior of the nanoparticle/surfactant systems.

Normally, both Triton X-100 and Pluronic-P123 are known as efficient CNT dispersing agents in deionized water. Triton X-100 molecule is composed of hydrophilic polyethylene oxide (PEO) group and a hydrophobic octyl group (Table S2, Supporting Information). This latter has a good affinity with the CNT  $sp^2$  structure through  $\pi$ - $\pi$  interactions between the CNT surface and the hydrophobic part of the surfactant. The hydrophilic part, by creating steric forces to counterbalance the van der Waals attractive forces between the CNTs, induces their stable dispersion in water. The Pluronic-P123 is a symmetric triblock copolymer with an alternating linear fashion: PEO-PPO-PEO comprising polyethylene oxide (PEO) as the hydrophilic component (like Triton X-100) and the hydrophobic group being a polypropylene oxide (PPO).

A typical scenario for steric stabilization relies on the dual action of the Pluronic-P123 thanks to a selective interaction with the solvent: while the hydrophobic block (PPO) is adsorbed by  $\pi$ - $\pi$  interactions on the nanotube outside wall, the hydrophilic block (PEO) dangles into the solvent and repels the other hydrophilic blocks via steric repulsions<sup>44,46,47</sup>. From the literature, it is explained that Pluronic-P123 is a greatly proved surfactant for CNTs in water and organic-based compounds, since these carbonaceous structure diameters ( $\approx 3$  nm) match with the Pluronic-P123 native micelle diameter (8 nm) favoring homogenous surfactant adsorption on the nanotube<sup>44,48-51</sup>. A proper nanotube coverage and subsequent good dispersion in deionized water was reported for an optimum CNT/surfactant weight ratio between 0.03 and 0.15 for Triton X-100<sup>44,48,52,53</sup> and between 0.02 and 0.14 for Pluronic-P123<sup>43,44,52,54</sup> which are quite similar optimum dispersion windows. Knowing that this optimum ratio window can be slightly modified depending on the

CNT type and probably the dispersing medium, for both Triton X-100 and Pluronic-P123, the surfactant concentration used in this work are roughly in the good dispersion CNT/dispersion ratio (Table 1). The poor dispersive behavior observed in the Triton X-100 based samples is therefore a possible consequence of the high ionic strength in the used copper ion solution, as argued in the following.

For ionic surfactants, the CMC is usually downshifted when the ionic strength increases in water; the screening effects due to the presence of ions in the vicinity of their charged heads reduce repulsive forces and favor their self-assembly under the form of micelles. For nonionic surfactants, similar effects have been reported<sup>55,56</sup>. For both Triton X-100 and Pluronic-P123, since the employed concentration is above the CMC (Table S2, Supporting Information), micelles are easily formed and the surfactants accumulate at the interfaces such as solvent/air interface. That means that, compared to pure water, the used copper ion solution would promote the formation of surfactant micelles for both Triton X-100 and Pluronic-P123. If the number of micelles is significantly increased in the copper ion solution compared to in deionized water, depletion attractive interactions are much more likely to occur and they will induce DWCNT re-agglomeration. DWCNT agglomerates are indeed observed for Triton X-100 samples even at quite a high DWCNT/Triton X-100 ratio (ST1). This depletion-flocculation of the DWCNTs occurs as Triton X-100 hydrophilic part (PEO) is not able to counterbalance the agglomeration interactions due to the micelle osmotic pressure. This could explain the observed DWCNT agglomerates in Figures 3a, 3b and 3c, leading to a poor DWCNT dispersion by Triton X-100. On the other hand, for Pluronic-P123, such destabilization phenomenon is only observed for the lower DWCNT/Pluronic-P123 ratio (SP1). A quite good sign of an efficient dispersion of DWCNTs is observed for the DWCNT/surfactant weight ratio between 0.1 and 0.05, meaning that additional

repulsive interactions certainly appear between the DWCNTs when Pluronic-P123 is used (Figures 3h and 3i).

Although both Triton X-100 and Pluronic-P123 are nonionic surfactants with PEO blocks as a hydrophilic agent, Triton X-100 has a linear structure containing 10 PEO molecules while Pluronic-P123 is formed by two PEO blocks, each one repeated containing 20 PEO molecules, giving to Pluronic-P123 the form of long-shaped chains. Targeting this structural difference, the hydrophilic-lipophilic balance (HLB) which measures the degree to which a surfactant is rather hydrophilic or lipophilic can be considered. Over a scale from 0 to 20, the lowest values of HLB correspond to hydrophobic molecules and vice versa. Triton X-100 and Pluronic-P123 have a HLB of 13.5 and 8, respectively. Pluronic-P123 being less hydrophilic than Triton X-100, it has a better affinity for the hydrophobic DWCNT surface and being larger than Triton X-100, it has a higher tendency to be adsorbed on the DWCNT surface<sup>50</sup>.

Figure 6 summarizes the DWCNT dispersion behavior when Pluronic-P123 or Triton X-100 is used as surfactant in the Cu<sup>2+</sup> ion solution. As Triton X-100 has a lower affinity for the hydrophobic DWCNTs, its desorption from the DWCNT surface is certainly much easier which could reduce the DWCNT coverage rate. Simultaneously, Triton X-100 likely forms micelles which number is expected to increase within the copper ion solution and be responsible for the appearance of the already mentioned depletion forces leading to DWCNT agglomeration (Figure 6a). These two effects are certainly combined resulting in the destabilization phenomenon observed over a large surfactant concentration range as Triton X-100 is used. On the contrary, as a proper amount of Pluronic-P123 is used, the Pluronic-P123 molecules remain adsorbed on the DWCNT surface and promote their dispersion by efficient steric repulsions between them (Figure 6b).

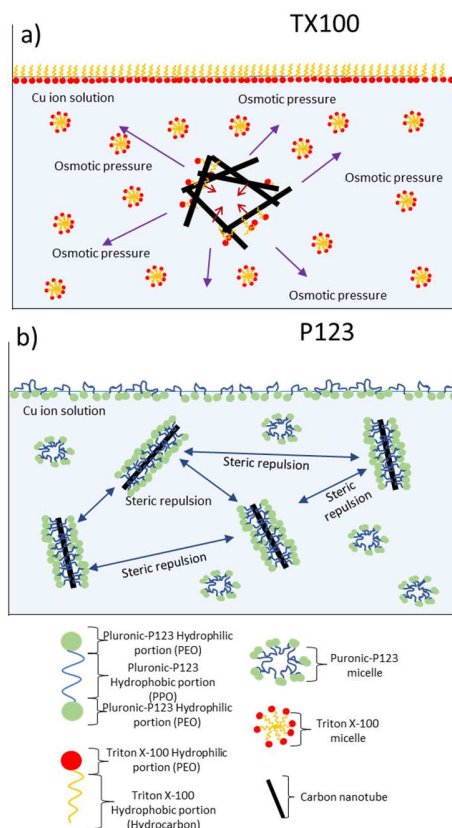


**Figure 6** Scenarios of DWCNTs in the Cu ion solution dispersed with a) Triton X-100 and dispersed with b) Pluronic-P123.

### 3.2 DWCNT/CU co-electrodeposition

#### 3.2.1 Preparation of CNT/Cu powders

The DWCNT dispersion obtained with 2.0 wt.% of Pluronic-P123 (SP3) was chosen to co-electrodeposit the DWCNTs and copper because the solution showed the best dispersive performance. Therefore, copper and DWCNT-copper deposits were fabricated using the chronopotentiometry technique by applying different constant current densities. At low current

densities ( $21.2 \text{ mA cm}^{-2}$ ), the deposits formed compact layers firmly attached to the surface of the copper cathode and impossible to remove. At high current densities ( $116 \text{ mA cm}^{-2}$ ), well-defined powders formed but also a large volume of oxygen on the Pt mesh electrode was generated which caused excessive foam escaping from the electrochemical cell. Therefore, an optimal current density was selected at  $-69.6 \text{ mA cm}^{-2}$ . Sample potential profiles registered for the copper electrodeposition from an electrolyte with and without additives and resulting copper/composite powders are shown in Figure 7. The fabricated DWCNT/Cu composite powders appeared to be relatively darker than the copper powders without CNTs.

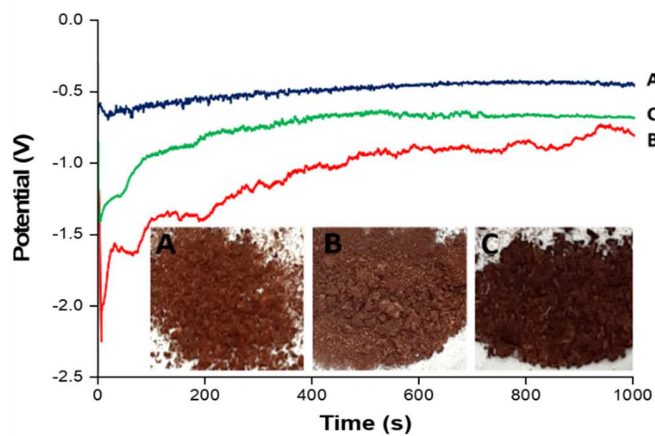


**Figure 7** Chronopotentiometric curves of the copper electrodeposition process, showing the variation of the electrode potential during the electrodeposition process at a deposition current density of  $-69.6 \text{ mA cm}^{-2}$ . The inset picture shows the powders resulting from each electrodeposition step. A)  $0.5 \text{ M CuSO}_4 / 0.05 \text{ M H}_2\text{SO}_4$  (pH 1); B)  $0.5 \text{ M CuSO}_4 / 0.05 \text{ M H}_2\text{SO}_4$  (pH 1) / 2 wt.% of P123; C)  $0.5 \text{ M CuSO}_4 / 0.05 \text{ M H}_2\text{SO}_4$  (pH 1) / 0.1 wt.% of DWCNT / 2 wt.% of P123.

Chronopotentiometric profile *A* obtained for the pure copper electrodeposition from the copper bath without additives shows the almost instant phase of higher overpotential, due to the nucleation of copper particles on the copper rod surface, followed by a growth of copper particles at constant potential after their nucleation.

Electrodeposition profiles obtained from the baths containing Pluronic-P123 (profile *B*) and DWCNT/Pluronic-P123 (profile *C*) are both characterized by an initial period of high potential and the following period of low deposition potential, the Pluronic-P123 requiring the lowest overall copper deposition potential. The high potential of the deposition observed at the beginning of each profile (-1.4 V and -2.0 V in presence of DWCNT/Pluronic-P123 and Pluronic-P123, respectively) may be linked to the wetting properties of Pluronic-P123 due to the presence of PEO segments known to decrease the surface tension of aqueous solutions <sup>57</sup>. Lower copper electrodeposition potentials for the baths containing the surfactants are caused by the adsorption of hydrophilic PEO ends of the surfactant on the metallic copper and partial blocking of the electrode surface. Simultaneously PEO can immobilize copper ions in the electrolyte by coordinating them with oxygen atoms slowing down their migration towards the electrode. These two effects inhibit the process of electrodeposition of copper.

The addition of DWCNTs to the copper/Pluronic-P123 electrolyte partially balances the inhibiting effect of surfactant and shifts the reduction potential of Cu toward a more positive value.

Various models were developed to describe the process of electrochemical synthesis of CNT composites with metals <sup>58,59</sup>. For an agitated solution of copper salt, DWCNT and Pluronic-P123 surfactant, the one proposed by Celis *et al.* is the most appropriate <sup>59</sup>. According to this model, well dispersed DWCNTs stabilized by hydrophobic moieties of Pluronic-P123 surfactant are carried toward the hydrodynamic boundary layer by magnetic stirring and through the diffusion



layer by diffusion toward the copper cathode. The hydrophilic parts of Pluronic-P123 loosely adsorb on the metallic surface of the electrode. DWCNTs remain in close vicinity of the electrode surface becoming effective nucleation centers for electrodeposited copper <sup>60</sup>.

### *3.2.2 Evidence of DWCNT presence within the electrodeposited copper matrix*

Raman spectroscopy is a powerful technique to characterize CNTs. Due to the resonant behavior of the one-dimensional CNTs, their Raman intensity is enhanced by several order of magnitudes compared to other non-resonant compounds offering an efficient sensor for CNTs. Raman spectroscopy is an obvious technique for CNT characterization, especially as it is sensitive to the type of CNTs and the presence of defects within their structure. In this work, three samples were studied by Raman spectroscopy: the raw and the purified DWCNTs and the prepared DWCNT/Cu composites (Figures 8a and 8b). For the 3 samples, the spectra show comparable features. Regarding the low-frequency domain, the radial breathing modes (RBM) show similar contributions which can be well assigned to DWCNTs. Below around 180  $\text{cm}^{-1}$ , the features are due to the external walls of the DWCNTs and above this frequency, the internal walls of the DWCNTs are contributing to the Raman signal. Moreover, thanks to the RBM, it is possible to estimate the internal diameter of the tubes <sup>61</sup>. The data in Figure 8a show an average internal diameter of 1.5 ( $\pm 0.15$ ) nm for the raw, purified DWCNT and the electrodeposited tubes. The average external diameter for the three tubes was 2 nm. These results agree with the TEM observations in Figures S1a and S1c, in Supporting Information. Typically, the G band (around 1590  $\text{cm}^{-1}$ ) is characteristic of the  $\text{sp}^2$  network formed by the double-bonded carbon atoms and the D band (around 1320-1330  $\text{cm}^{-1}$ ) is related to “disorder” or defects when the hybridization of carbon atoms turns to  $\text{sp}^3$  through damaging or functionalization. The ratio  $I_D/I_G$  is another

important parameter found from Raman spectroscopy.  $I_D/I_G$  gives a qualitative parameter related to the structural defects which are introduced in the DWCNTs during the purification and co-electrodeposition process. The intensity of the D band can be directly compared for the 3 spectra which have been normalized by the G band intensity in Figure 8b.  $I_D/I_G$  is around  $0.14 (\pm 0.01)$ ,  $0.18 (\pm 0.02)$  and  $0.22 (\pm 0.03)$  for the raw, purified and DWCNTs implanted in the copper matrix, respectively.  $I_D/I_G$  of the purified DWCNTs is close to that of the raw DWCNTs meaning that the purification treatment well preserves the CNT structure in agreement with previous works<sup>30,62</sup>. In the same way, when comparing  $I_D/I_G$  of the purified DWCNTs before and after their incorporation within the copper matrix, no clear modification is noticeable in agreement with the soft character of the electrodeposition process.

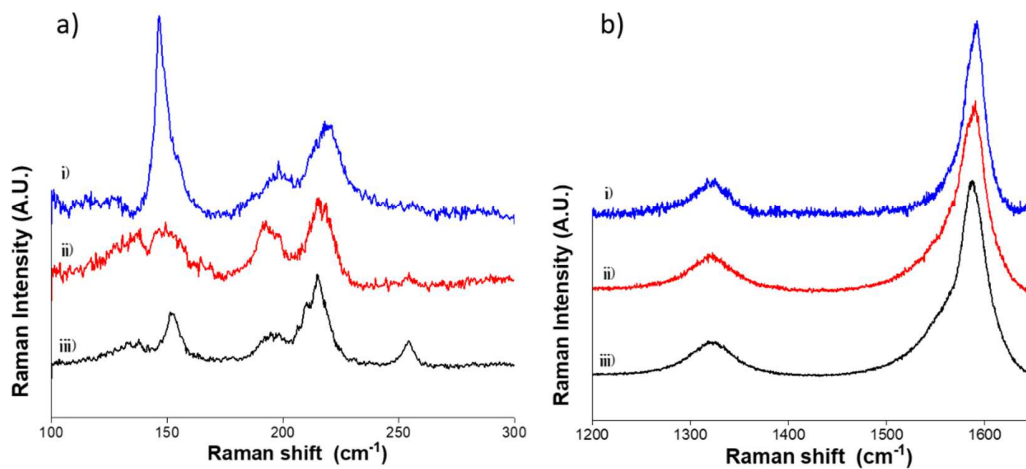


**Figure 8** Raman spectra of i) DWCNT/Cu composite, ii) Purified DWCNTs and iii) Raw DWCNTs; a) RBM spectral domain and b) D and G band spectral domain.

TGA is considered as an important technique to study carbonaceous nanomaterials as it can help to evaluate their amount in a composite material. Indeed, under oxygen or air, the CNTs burn off

above their combustion temperature typically in the 300-600 °C range. The combustion temperature for the used DWCNTs is around 450 °C (Figure S1b, Supporting Information). The metallic part of the CNT/metal mixture will be oxidized during TGA. Moreover, this metallic nature of copper is evidenced by X-ray diffraction shown in Figure S3, in Supporting Information. In Figure 9, the thermograms show that the weight gained in % due to copper oxidation is higher for copper alone (24.8 % and 22.6 % for copper alone and DWCNT/Cu, respectively). Assuming that the copper oxide is CuO, the expected weight gain due to oxidation can be evaluated by calculating the difference in weight when CuO is formed from Cu ( $\text{Cu} + \text{O} \rightarrow \text{CuO}$ ) by dividing the molecular weight of oxygen by that of copper *i.e.*  $16/63.55 \times 100 = 25.2 \%$ , which is in very good agreement with the 24.8 % measured by TGA. Considering, the reduced amount of copper in the CNT/Cu mixture (composite), the content of CNTs in wt.%,  $X_{CNT}$ , from the values measured by TGA, can be determined by the following relation:

$$22.6 = 24.8 - X_{CNT} - (24.8 (1 - X_{CNT}))$$

Which means that the composite contains 1.13 wt.% of CNTs which corresponds to 4.9 vol.%. Under the used conditions, the performed co-electrodeposition is efficient to incorporate a significant amount of CNT in the copper matrix.

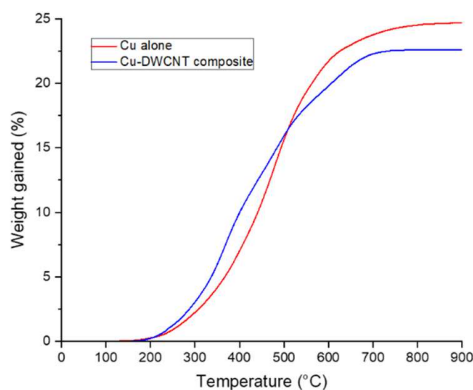


**Figure 9** Thermograms under dry air of pure copper and the DWCNT/Cu composite by electrodeposition.

The prepared composites materials were observed by SEM and TEM and typical images are shown in Figures 10a and 10b and Figures 10c and 10d, respectively. During both SEM and TEM observations, the CNTs can be easily observed everywhere within the copper matrix. From SEM, CNTs do not form the typically observed large agglomerates when they tend to separate from the surrounding medium; they are well distributed and embedded within the copper matrix.

From TEM micrographs (Figures 10c and 10d), the DWCNTs are noticeable coming out from the copper particles, revealing that the DWCNTs and copper are closely connected together.

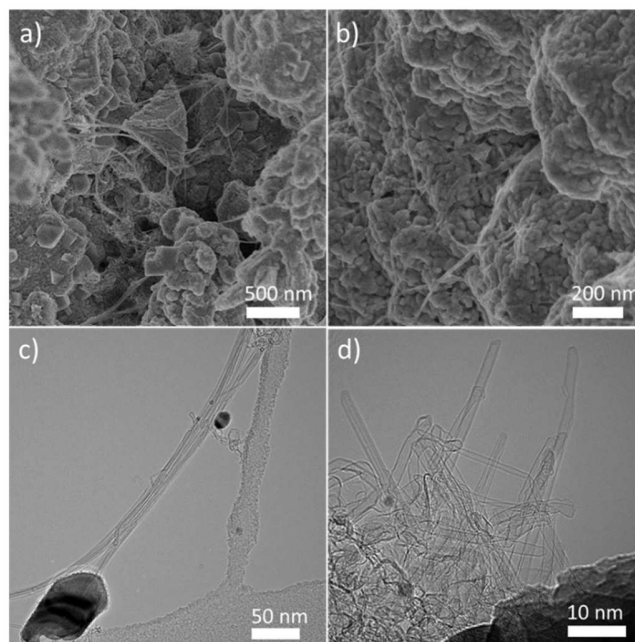


**Figure 10** SEM (a and b) and TEM (c and d) images of the DWCNT/Cu composite prepared by co-electrodeposition.

## **Conclusion**

DWCNTS were firstly purified by a one-pot gas-phase and highly-selective chlorine-based thermal purification treatment. Secondly, 9 samples were prepared. They contain different amounts of DWCNTs and Triton X-100, SDS or Pluronic-P123 as surfactants in a copper ion solution. The success of Pluronic-P123 and failure of both Triton X-100 and SDS surfactant was unanticipated as these last are both well recognized for their success to disperse CNTs in standard deionized water. The poor solubility of SDS propitiated heterogeneous samples, making them not reliable for the purpose of the present work. In the case of the nonionic surfactants, based on their chemical difference and especially the HLB, depletion was proposed as a possible mechanism responsible of the observed re-agglomeration of the tubes when Triton X-100 was used as surfactant in the copper ion solution. Pluronic-P123 showed the best DWCNT affinity and therefore the best dispersive power and stable and homogenous DWCNT dispersion could be successfully prepared in this particularly high ionic strength solution thanks to efficient steric forces. This work represents important advances in CNT/Cu composites since high-quality dispersions of DWCNTs could be successfully achieved in high ionic strength copper electrolytes. For future works, the study of the DWCNT's influence in the growth and resulting morphology of the Cu grains is strongly suggested regarding the interest in their use as current carriers. Additionally, a broad study of the composite material properties is foresight for the future development of this technology.

## AUTHOR INFORMATION

### Corresponding Author

\*Brigitte Vigolo (B.V.); [Brigitte.Vigolo@univ-lorraine.fr](mailto:Brigitte.Vigolo@univ-lorraine.fr)

### Author Contributions

The manuscript was written through contributions of all authors. All authors have given approval to the final version of the manuscript.

## ACKNOWLEDGMENT

This work was supported by Partenariats Hubert Curien (PHC)/Campus France, PHC ALLIANCE 2019 43237NB. The authors would like to thank the platforms “Microscopies, Microprobes and Metallography (3M)”, “X- $\gamma$ ” and “Optics and Laser” (Institut Jean Lamour, IJL, Nancy, France) for facilities access, Jaafar Ghanbaja and Sébastien Hupont for their valuable help for TEM and Raman spectroscopy experiments, respectively. B. Vigolo and M. Pavía thanks Lionel Aranda for his help during TGA experiments.

## REFERENCES

- (1) Rho, H.; Park, M.; Park, M.; Park, J.; Han, J.; Lee, A.; Bae, S.; Kim, T.-W.; Ha, J.-S.; Kim, S. M.; Lee, D. S.; Lee, S. H. Metal Nanofibrils Embedded in Long Free-Standing Carbon Nanotube Fibers with a High Critical Current Density. *NPG Asia Mater* **2018**, *10* (4), 146–155. <https://doi.org/10.1038/s41427-018-0028-3>.
- (2) Han, B.; Guo, E.; Xue, X.; Zhao, Z.; Luo, L.; Qu, H.; Niu, T.; Xu, Y.; Hou, H. Fabrication and Densification of High Performance Carbon Nanotube/Copper Composite Fibers. *Carbon* **2017**, *123*, 593–604. <https://doi.org/10.1016/j.carbon.2017.08.004>.
- (3) Seichepine, F.; Flahaut, E.; Vieu, C. A Simple and Versatile Method for Statistical Analysis of the Electrical Properties of Individual Double Walled Carbon Nanotubes. *Microelectronic Engineering* **2011**, *88* (7), 1637–1639. <https://doi.org/10.1016/j.mee.2011.01.081>.
- (4) Mousavi, Z.; Heuzey, M.-C.; Kamal, M. R.; Flahaut, E.; Carreau, P. J. Rheological, Electrical, and Dynamic Thermomechanical Properties: Comparison between Multiwall and Double-Wall Carbon Nanotubes in Polylactide and Polyamide 11. *Physics of Fluids* **2021**, *33* (11), 113103. <https://doi.org/10.1063/5.0068537>.
- (5) Venkataraman, A.; Amadi, E. V.; Chen, Y.; Papadopoulos, C. Carbon Nanotube Assembly

- and Integration for Applications. *Nanoscale Research Letters* **2019**, *14* (1), 220. <https://doi.org/10.1186/s11671-019-3046-3>.
- (6) Yekeen, N.; Xin Kun, T.; Al-Yaseri, A.; Sagala, F.; Kamal Idris, A. Influence of Critical Parameters on Nanoparticles-Surfactant Stabilized CO<sub>2</sub> Foam Stability at Sub-Critical and Supercritical Conditions. *Journal of Molecular Liquids* **2021**, *338*, 116658. <https://doi.org/10.1016/j.molliq.2021.116658>.
  - (7) Hannula, P.-M.; Peltonen, A.; Aromaa, J.; Janas, D.; Lundström, M.; Wilson, B. P.; Koziol, K.; Forsén, O. Carbon Nanotube-Copper Composites by Electrodeposition on Carbon Nanotube Fibers. *Carbon* **2016**, *107*, 281–287. <https://doi.org/10.1016/j.carbon.2016.06.008>.
  - (8) Vishwanath, K.; Raji, G.; Shakiba, A.; Murthy, S. K. V. Mechanical Properties of Copper Nanocomposites Reinforced with Uncoated and Nickel Coated Carbon Nanotubes. *FME Transactions* **2018**, *46* (4). <https://doi.org/10.5937/fmet1804623k>.
  - (9) Arnaud, C.; Lecouturier, F.; Mesguich, D.; Ferreira, N.; Chevallier, G.; Estournès, C.; Weibel, A.; Laurent, C. High Strength – High Conductivity Double-Walled Carbon Nanotube – Copper Composite Wires. *Carbon* **2016**, *96*, 212–215. <https://doi.org/10.1016/j.carbon.2015.09.061>.
  - (10) Nayan, N.; Shukla, A. K.; Chandran, P.; Bakshi, S. R.; Murty, S. V. S. N.; Pant, B.; Venkitakrishnan, P. V. Processing and Characterization of Spark Plasma Sintered Copper/Carbon Nanotube Composites. *Materials Science and Engineering: A* **2017**, *682*, 229–237. <https://doi.org/10.1016/j.msea.2016.10.114>.
  - (11) Mendoza, M. E.; Solórzano, I. G.; Brocchi, E. A. Mechanical and Electrical Characterization of Cu-2wt.% SWCNT Nanocomposites Synthesized by in Situ Reduction. *Materials Science and Engineering: A* **2012**, *544*, 21–26. <https://doi.org/10.1016/j.msea.2012.02.052>.
  - (12) Lim, B.; Kim, C.; Kim, B.; Shim, U.; Oh, S.; Sung, B.; Choi, J.; Baik, S. The Effects of Interfacial Bonding on Mechanical Properties of Single-Walled Carbon Nanotube Reinforced Copper Matrix Nanocomposites. *Nanotechnology* **2006**, *17* (23), 5759–5764. <https://doi.org/10.1088/0957-4484/17/23/008>.
  - (13) Wang, Z.; Cai, X.; Yang, C.; Zhou, L.; Hu, C. An Electrodeposition Approach to Obtaining Carbon Nanotubes Embedded Copper Powders for the Synthesis of Copper Matrix Composites. *Journal of Alloys and Compounds* **2018**, *735*, 1357–1362. <https://doi.org/10.1016/j.jallcom.2017.11.255>.
  - (14) Sharma, V. M.; Maity, D.; Racherla, V.; Pal, S. K. Friction Sintering of Copper Powder Using a New Rapid, Cost Effective and Energy Efficient Process. In *V004T03A008*; American Society of Mechanical Engineers: College Station, Texas, USA, 2018. <https://doi.org/10.1115/MSEC2018-6684>.
  - (15) Gao, Z.; Zuo, T.; Wang, M.; Zhang, L.; Da, B.; Ru, Y.; Xue, J.; Wu, Y.; Han, L.; Xiao, L. In-Situ Graphene Enhanced Copper Wire: A Novel Electrical Material with Simultaneously High Electrical Conductivity and High Strength. *Carbon* **2022**, *186*, 303–312. <https://doi.org/10.1016/j.carbon.2021.10.015>.
  - (16) Arai, S.; Ozawa, M.; Shimizu, M. Fabrication of Three-Dimensional (3D) Copper/Carbon Nanotube Composite Film by One-Step Electrodeposition. *J. Electrochem. Soc.* **2016**, *163* (14), D774–D779. <https://doi.org/10.1149/2.0601614jes>.
  - (17) Jayathilaka, W. a. D. M.; Chinnappan, A.; Ramakrishna, S. A Review of Properties Influencing the Conductivity of CNT/Cu Composites and Their Applications in Wearable/Flexible Electronics. *J. Mater. Chem. C* **2017**, *5* (36), 9209–9237. <https://doi.org/10.1039/c7tc02965a>.
  - (18) Bazbouz, M. B.; Aziz, A.; Copic, D.; De Volder, M.; Welland, M. E. Fabrication of High Specific Electrical Conductivity and High Ampacity Carbon Nanotube/Copper Composite

- Wires. *Adv. Electron. Mater.* **2021**, *7* (4). <https://doi.org/10.1002/aelm.202001213>.
- (19) Raja, P. M. V.; Esquenazi, G. L.; Gowenlock, C. E.; Jones, D. R.; Li, J.; Brinson, B.; Barron, A. R. Electrodeposition of Cu-SWCNT Composites. *Journal of Carbon Research C* **2019**, *5* (3). <https://doi.org/10.3390/c5030038>.
  - (20) Kazimierska, E.; Andreoli, E.; Barron, A. R. Understanding the Effect of Carbon Nanotube Functionalization on Copper Electrodeposition. *J Appl Electrochem* **2019**, *49* (8), 731–741. <https://doi.org/10.1007/s10800-019-01318-x>.
  - (21) Arai, S.; Saito, T.; Endo, M. Cu-MWCNT Composite Films Fabricated by Electrodeposition. *J. Electrochem. Soc.* **2010**, *157* (3), D147. <https://doi.org/10.1149/1.3280034>.
  - (22) Banerjee, S.; Hemraj-Benny, T.; Wong, S. S. Covalent Surface Chemistry of Single-Walled Carbon Nanotubes. *Adv. Mater.* **2005**, *17* (1), 17–29. <https://doi.org/10.1002/adma.200401340>.
  - (23) Hirsch, A. Functionalization of Single-Walled Carbon Nanotubes. *Angew. Chem.-Int. Edit.* **2002**, *41* (11), 1853–1859. [https://doi.org/10.1002/1521-3773\(20020603\)41:11<1853::AID-ANIE1853>3.0.CO;2-N](https://doi.org/10.1002/1521-3773(20020603)41:11<1853::AID-ANIE1853>3.0.CO;2-N).
  - (24) Peng, X.; Wong, S. S. Functional Covalent Chemistry of Carbon Nanotube Surfaces. *Adv. Mater.* **2009**, *21* (6), 625–642. <https://doi.org/10.1002/adma.200801464>.
  - (25) Wang, S. Optimum Degree of Functionalization for Carbon Nanotubes. *Curr. Appl. Phys.* **2009**, *9* (5), 1146–1150. <https://doi.org/10.1016/j.cap.2009.01.004>.
  - (26) Singh, S.; Kruse, P. Carbon Nanotube Surface Science. *Int. J. Nanotechnol.* **2008**, *5* (9–12), 900–929. <https://doi.org/10.1504/IJNT.2008.019826>.
  - (27) Roslyk, I.; Stovpchenkoko, G.; Galchenko, G. Influence of Surfactants on Copper-CNTs Electrodeposition. *Chemistry & Chemical Technology* **2021**, *15* (1), 125–131. <https://doi.org/10.23939/chcht15.01.125>.
  - (28) Jung, J.; Hyun Suh, E.; Jeong, Y.; Yun, D.-J.; Chan Park, S.; Gyu Oh, J.; Jang, J. Ionic-Liquid Doping of Carbon Nanotubes with [HMIM][BF<sub>4</sub>] for Flexible Thermoelectric Generators. *Chemical Engineering Journal* **2022**, *438*, 135526. <https://doi.org/10.1016/j.cej.2022.135526>.
  - (29) Flahaut, E.; Bacsá, R.; Peigney, A.; Laurent, C. Gram-Scale CCVD Synthesis of Double-Walled Carbon Nanotubes. *Chem. Commun.* **2003**, No. 12, 1442. <https://doi.org/10.1039/b301514a>.
  - (30) Desforges, A.; Bridi, A. V.; Kadok, J.; Flahaut, E.; Le Normand, F.; Gleize, J.; Bellouard, C.; Ghanbaja, J.; Vigolo, B. Dramatic Enhancement of Double-Walled Carbon Nanotube Quality through a One-Pot Tunable Purification Method. *Carbon* **2016**, *110*, 292–303. <https://doi.org/10.1016/j.carbon.2016.09.033>.
  - (31) Rastogi, R.; Kaushal, R.; Tripathi, S. K.; Sharma, A. L.; Kaur, I.; Bharadwaj, L. M. Comparative Study of Carbon Nanotube Dispersion Using Surfactants. *Journal of Colloid and Interface Science* **2008**, *328* (2), 421–428. <https://doi.org/10.1016/j.jcis.2008.09.015>.
  - (32) Raiah, K.; Djalab, A.; Hadj-Ziane-Zafour, A.; Soula, B.; Galibert, A.-M.; Flahaut, E. Influence of the Hydrocarbon Chain Length of Imidazolium-Based Ionic Liquid on the Dispersion and Stabilization of Double-Walled Carbon Nanotubes in Water. *Colloid Surf. A-Physicochem. Eng. Asp.* **2015**, *469*, 107–116. <https://doi.org/10.1016/j.colsurfa.2015.01.015>.
  - (33) Berrada, N.; Desforges, A.; Bellouard, C.; Flahaut, E.; Gleize, J.; Ghanbaja, J.; Vigolo, B. Protecting Carbon Nanotubes from Oxidation for Selective Carbon Impurity Elimination. *J. Phys. Chem. C* **2019**, *123* (23), 14725–14733. <https://doi.org/10.1021/acs.jpcc.8b12554>.
  - (34) Desforges, A.; Bridi, A. V.; Kadok, J.; Flahaut, E.; Le Normand, F.; Gleize, J.; Bellouard, C.; Ghanbaja, J.; Vigolo, B. Dramatic Enhancement of Double-Walled Carbon Nanotube Quality through a One-Pot Tunable Purification Method. *Carbon* **2016**, *110*, 292–303. <https://doi.org/10.1016/j.carbon.2016.09.033>.
  - (35) Mercier, G.; Herold, C.; Mareche, J.-F.; Cahen, S.; Gleize, J.; Ghanbaja, J.; Lamura, G.;



- Bellouard, C.; Vigolo, B. Selective Removal of Metal Impurities from Single Walled Carbon Nanotube Samples. *New J. Chem.* **2013**, *37* (3), 790–795. <https://doi.org/10.1039/c2nj41057e>.
- (36) Mercier, G.; Mareche, J.-F.; Cahen, S.; Herold, C.; Vigolo, B. Méthode De Purification De Nanotubes De Carbone, May 3, 2012. <https://patentscope.wipo.int/search/fr/detail.jsf?docId=WO2012056184> (accessed 2021-12-13).
- (37) Berrada, N.; El Housseini, W.; Desforges, A.; Gleize, J.; Ghanbaja, J.; Etienne, M.; Houlle, M.; Bellouard, C.; Vigolo, B. Multiwalled Carbon Nanotube Purification Probed by Electrochemistry: Low-Temperature Chlorine Gas Treatment Meets High-Temperature Annealing. *ChemNanoMat* **2022**, *8* (10), e202200275. <https://doi.org/10.1002/cnma.202200275>.
- (38) Vigolo, B.; Penicaud, A.; Coulon, C.; Sauder, C.; Pailler, R.; Journet, C.; Bernier, P.; Poulin, P. Macroscopic Fibers and Ribbons of Oriented Carbon Nanotubes. *Science* **2000**, *290* (5495), 1331–1334. <https://doi.org/10.1126/science.290.5495.1331>.
- (39) Krittayavathananon, A.; Li, X.; Batchelor-McAuley, C.; Sawangphruk, M.; Compton, R. G. Comparing the Effect of Different Surfactants on the Aggregation and Electrical Contact Properties of Graphene Nanoplatelets. *Applied Materials Today* **2018**, *12*, 163–167. <https://doi.org/10.1016/j.apmt.2018.04.007>.
- (40) Mazrouaa, A. M.; Mansour, N. A.; Abed, M. Y.; Youssif, M. A.; Shenashen, M. A.; Awual, Md. R. Nano-Composite Multi-Wall Carbon Nanotubes Using Poly(p-Phenylene Terephthalamide) for Enhanced Electric Conductivity. *Journal of Environmental Chemical Engineering* **2019**, *7* (2), 103002. <https://doi.org/10.1016/j.jece.2019.103002>.
- (41) Mubasher; Mumtaz, M.; Lashari, N. U. R.; Hassan, M.; Tangsee, S.; Khan, M. T. Multi-Walled Carbon Nanotubes and Chromium Ferrites Nanoparticles Nanohybrids as Anode Materials for Lithium-Ion Batteries. *Journal of Alloys and Compounds* **2021**, *872*, 159654. <https://doi.org/10.1016/j.jallcom.2021.159654>.
- (42) Palladino, P.; Ragone, R. Ionic Strength Effects on the Critical Micellar Concentration of Ionic and Nonionic Surfactants: The Binding Model. *Langmuir* **2011**, *27* (23), 14065–14070. <https://doi.org/10.1021/la202897q>.
- (43) Vigolo, B.; Hérold, C. Processing Carbon Nanotubes. In *Carbon Nanotubes-Synthesis, Characterization, Applications*; InTech, 2011; pp 3–28.
- (44) Schott, H. Comparing the Surface Chemical Properties and the Effect of Salts on the Cloud Point of a Conventional Nonionic Surfactant, Octoxynol 9 (Triton X-100), and of Its Oligomer, Tyloxapol (Triton WR-1339). *Journal of Colloid and Interface Science* **1998**, *205* (2), 496–502. <https://doi.org/10.1006/jcis.1998.5721>.
- (45) Lavagna, L.; Nisticò, R.; Musso, S.; Pavese, M. Functionalization as a Way to Enhance Dispersion of Carbon Nanotubes in Matrices: A Review. *Materials Today Chemistry* **2021**, *20*, 100477. <https://doi.org/10.1016/j.mtchem.2021.100477>.
- (46) Mallakpour, S.; Soltanian, S. Surface Functionalization of Carbon Nanotubes: Fabrication and Applications. *RSC Adv.* **2016**, *6* (111), 109916–109935. <https://doi.org/10.1039/C6RA24522F>.
- (47) Girard, L.; Naskar, B.; Dufrêche, J.-F.; Lai, J.; Diat, O.; Bauduin, P. A Thermodynamic Model of Non-Ionic Surfactants' Micellization in the Presence of Polyoxometalates. *Journal of Molecular Liquids* **2019**, *293*, 111280. <https://doi.org/10.1016/j.molliq.2019.111280>.
- (48) Kang, Y.; Taton, T. A. Micelle-Encapsulated Carbon Nanotubes: A Route to Nanotube Composites. *J. Am. Chem. Soc.* **2003**, *125* (19), 5650–5651. <https://doi.org/10.1021/ja034082d>.
- (49) Shvartzman-Cohen, R.; Nativ-Roth, E.; Baskaran, E.; Levi-Kalishman, Y.; Szleifer, I.; Yerushalmi-Rozen, R. Selective Dispersion of Single-Walled Carbon Nanotubes in the

- Presence of Polymers: The Role of Molecular and Colloidal Length Scales. *JACS* **2004**, *126* (45), 14850–14857. <https://doi.org/10.1021/jao46377c>.
- (50) Shvartzman-Cohen, R.; Monje, I.; Florent, M.; Frydman, V.; Goldfarb, D.; Yerushalmi-Rozen, R. Self-Assembly of Amphiphilic Block Copolymers in Dispersions of Multiwalled Carbon Nanotubes As Reported by Spin Probe Electron Paramagnetic Resonance Spectroscopy. *Macromolecules* **2010**, *43* (2), 606–614. <https://doi.org/10.1021/ma9019398>.
- (51) Hamze, S.; Berrada, N.; Desforges, A.; Vigolo, B.; Gleize, J.; Ghanbaja, J.; Maré, T.; Cabaleiro, D.; Estellé, P. Dynamic Viscosity of Purified Multi-Walled Carbon Nanotubes Water and Water-Propylene Glycol-Based Nanofluids. *Heat Transfer Engineering* **2021**, *42* (19–20), 1663–1674. <https://doi.org/10.1080/01457632.2020.1818382>.
- (52) Wang, Y.; Gao, L.; Sun, J.; Liu, Y.; Zheng, S.; Kajiura, H.; Li, Y.; Noda, K. An Integrated Route for Purification, Cutting and Dispersion of Single-Walled Carbon Nanotubes. *Chemical Physics Letters* **2006**, *432* (1–3), 205–208. <https://doi.org/10.1016/j.cplett.2006.10.054>.
- (53) Yu, J.; Grossiord, N.; Koning, C. E.; Loos, J. Controlling the Dispersion of Multi-Wall Carbon Nanotubes in Aqueous Surfactant Solution. *Carbon* **2007**, *45* (3), 618–623. <https://doi.org/10.1016/j.carbon.2006.10.010>.
- (54) Shvartzman-Cohen, R.; Florent, M.; Goldfarb, D.; Szleifer, I.; Yerushalmi-Rozen, R. Aggregation and Self-Assembly of Amphiphilic Block Copolymers in Aqueous Dispersions of Carbon Nanotubes. *Langmuir* **2008**, *24* (9), 4625–4632. <https://doi.org/10.1021/la703782g>.
- (55) Goh, P.; Ng, B.; Aziz, M.; Sanip, S. Surfactant Dispersed Multi-Walled Carbon Nanotube/Polyetherimide Nanocomposite Membrane. *Solid State Sci.* **2010**, *12* (12), 2155–2162. <https://doi.org/10.1016/j.solidstatesciences.2010.09.017>.
- (56) Keinänen, P.; Siljander, S.; Koivula, M.; Sethi, J.; Sarlin, E.; Vuorinen, J.; Kanerva, M. Optimized Dispersion Quality of Aqueous Carbon Nanotube Colloids as a Function of Sonochemical Yield and Surfactant/CNT Ratio. *Heliyon* **2018**, *4* (9), e00787. <https://doi.org/10.1016/j.heliyon.2018.e00787>.
- (57) Zanellato, G.; Schiavi, P. G.; Zononi, R.; Rubino, A.; Altimari, P.; Pagnanelli, F. Electrodeposited Copper Nanocatalysts for CO<sub>2</sub> Electroreduction: Effect of Electrodeposition Conditions on Catalysts' Morphology and Selectivity. *Energies* **2021**, *14* (16), 5012. <https://doi.org/10.3390/en14165012>.
- (58) Guglielmi, N. Kinetics of the Deposition of Inert Particles from Electrolytic Baths. *J. Electrochem. Soc.* **1972**, *119* (8), 1009. <https://doi.org/10.1149/1.2404383>.
- (59) Celis, J. P.; Roos, J. R.; Buelens, C. A Mathematical Model for the Electrolytic Codeposition of Particles with a Metallic Matrix. *J. Electrochem. Soc.* **1987**, *134* (6), 1402–1408. <https://doi.org/10.1149/1.2100680>.
- (60) Wang, Z.; Cai, X.; Yang, C.; Zhou, L. Improving Strength and High Electrical Conductivity of Multi-Walled Carbon Nanotubes/Copper Composites Fabricated by Electrodeposition and Powder Metallurgy. *Journal of Alloys and Compounds* **2018**, *735*, 905–913. <https://doi.org/10.1016/j.jallcom.2017.11.200>.
- (61) Osswald, S.; Flahaut, E.; Gogotsi, Y. In Situ Raman Spectroscopy Study of Oxidation of Double- and Single-Wall Carbon Nanotubes. *Chem. Mat.* **2006**, *18* (6), 1525–1533. <https://doi.org/10.1021/cm052755g>.
- (62) Berrada, N.; Desforges, A.; Bellouard, C.; Flahaut, E.; Gleize, J.; Ghanbaja, J.; Vigolo, B. Protecting Carbon Nanotubes From Oxidation for Selective Carbon Impurity Elimination. *J. Phys. Chem. C.* **2019**, *123* (23), 14725–14733. <https://doi.org/10.1021/acs.jpcc.8b12554>.

## TABLE OF CONTENTS

